Masonry Simulations Using Cohesion Parameter as Code Enrichment for a Non-standard Limit Analysis Approach

Bledian Nela[1,a*], Marco Pingaro[1,b], Alejandro Jiménez Rios[1,c], Emanuele Reccia[2,d] and Patrizia Trovalusci[1,e]

[1]Department of Structural and Geotechnical Engineering, Sapienza University of Rome, Italy

[2]Department of Civil Engineering, Environment and Architecture, University of Cagliari, Italy

[a]bledian.nela@uniroma1.it, [b]marco.pingaro@uniroma1.it, [c]alejandro.jimenezrios@uniroma1.it, [d]emanuele.reccia@unica.it, [e]patrizia.trovalusci@uniroma1.it

Keywords: Limit Analysis, Friction, No-tension contacts, Cohesion, Reinforced masonry arches.

Abstract. A significant number of scientific research groups are still nowadays dealing with masonry material as the main focus of study since it provides an open field of research that is far from resolution in a standardized manner. As masonry structures are highly vulnerable to any level of natural hazards, especially seismic activity, both traditional and composite materials have been used as reinforcements in masonry and provide different solutions that meet the key requirements set out by cultural heritage organizations. Extensive effort has gone into developing appropriate techniques of assessment, that usually demand an individualized methodology of analysis that is to be handled through comparative studies that require results validation. A very appealing field of study is the Limit Analysis approach towards masonry structures, as it offers quite accurate and, more importantly, robust results regarding this necessity to resolve the many diversities involved in the masonry numerical representation to achieve the outcomes required for the assessment. The enrichment of a limit analysis homemade code with the inclusion of diffused cohesion and frictional behaviour at the interface level is able to account, in a simplified but very robust manner, the perplexing issues involved with the numerical assessment of reinforced masonry structures. The cohesion incorporation is calibrated for a variety of in-plane applications, accounting for the joints' indirect tensile strength, that is able to simulate the strengthening measures. Results obtained are validated with literature and included in a comparative study between discrete numerical models that utilize different modelling strategies.

Introduction

The structural behaviour and response of masonry is a challenging task considering its composite nature as a material. In recent years a significant amount of interest has been given by diverse authors into tackling this issue [1, 2, 3, 4]. Among a large variety of methods and approaches, Limit Analysis (LA) has stood out as a rather simple but powerful method, compared to other approaches in the assessment of existing masonry structures [5, 6, 7]. LA involves a discrete modelling approach of masonry units as rigid blocks with joints unable to carry tension and resistant to sliding by friction that account for dry joints or joints with very weak mortar. It has been proven to be especially useful due to the following advantages:

- It enables micro modelling of every block and thus allows considering the geometrical scale influence on the structural response.
- It requires a relatively simple mechanical constitutive model and few input parameters with no need of extensive testing for material characterization.
- It provides straightforward results in terms of collapse multipliers and collapse mechanisms.

Recently, ALMA 2.0 (an inhouse LA software developed at Sapienza University of Rome) has been enriched with the possibility of assigning different values of cohesion to every joint in order to be able to account for tensile and shear strength of the joints. This feature is an addition to the various

already available software capabilities, namely, foundation settlement [7] and retrofitting tie modelling [8]. ALMA 2.0 is based on the theoretical background developed in [9]. The software solves the linear programming (LP) kinematic upper bound problem formulated in Eq. (1-4), in which associativity and normality rules are assumed.

$$\text{minimize:} \quad \alpha_c = \{\boldsymbol{\lambda}^T[\boldsymbol{c} - (\boldsymbol{A}_0\,\boldsymbol{N}_1)^T\boldsymbol{f}_0]\}. \tag{1}$$

$$\text{subjected to:} \quad (\boldsymbol{A}\,\boldsymbol{N}_1 - \boldsymbol{N}_2)\,\boldsymbol{\lambda} = \boldsymbol{0}. \quad \text{(compatibility condition)} \tag{2}$$

$$\boldsymbol{\lambda}^T\,(\boldsymbol{A}_0\,\boldsymbol{N}_1)^T\,\boldsymbol{f}_L - 1 = 0. \quad \text{(positive live load)} \tag{3}$$

$$\boldsymbol{\lambda} \geq \boldsymbol{0}. \tag{4}$$

In the above equations the unknown of the problem remains α_c, a scalar, as the collapse multiplier with $\boldsymbol{\lambda}$ as the plastic multiplier vector that contains the nonnegative coefficients. $\mathbf{A}_0$ is the inverse matrix of the compatibility kinematical submatrix $\mathbf{B}_1$ of maximum rank while the rest of the kinematical matrix $\mathbf{B}_2$ is stored in the $\mathbf{A}$ matrix as $\mathbf{A} = \mathbf{B}_2\,\mathbf{B}_1^{-1}$. $\mathbf{N}_1$ and $\mathbf{N}_2$ are the submatrices of the block-diagonal gradient matrix $\mathbf{N}$ and correspond to the submatrix of independent and linearly dependent kinematical variables, respectively. $\mathbf{f}_0$ and $\mathbf{f}_L$ are the vectors of the generalized actions on the centres of the blocks for the dead and live loads, respectively. Additional details on the derivations and formulation of the LP problem can be consulted in [9]. Different cohesion values can be assigned to every joint of the masonry assemblage. These values are stored in the form of a vector $\mathbf{c}$. A Mohr-Coulomb classical yield domain is considered with the inclusion of cohesion, thus indirectly involving tensile strength of the joints as $\boldsymbol{\sigma}_t = \mathbf{c}/\tan\phi$, for $\boldsymbol{\sigma}_t$ as the tensile strength and ϕ as the friction angle. After some algebraic operations the $\mathbf{c}$ vector is stored in the objective function to be minimized through LP.

The new capability of ALMA 2.0 has been exploited in this paper to simulate the reinforcement of masonry arches by utilizing increased cohesion values as a method for joint reinforcement. Several authors have studied the reinforcement of arches with composite materials. In particular [10, 11, 12] used partial and distributed reinforcements for arch strengthening. In order to validate the ability of ALMA 2.0 to reproduce the strengthening effect of such reinforcements in masonry arches, two examples have been chosen from literature, namely EX_1 and EX_2. The first example (EX_1) was originally published by Orduña [13] and then numerically reproduced using different modelling approaches (FEM, DEM and analytical) by Baraldi et al. [12] in order to apply and assess the effect of partial reinforcement. The second example (EX_2) is based on the extensive experimental campaign performed by Oliveira et al. [11] whose main objective, among others, was to provide results that may be used as calibration/validation benchmarks for numerical models of composite reinforced masonry arches.

EX_1 – Example 1 from Orduña [13]

This example consists of a semi-circular arch with an internal radius of 2.35 m and a ring thickness of 0.3 m which is divided into 31 voussoirs (see Fig. 1). The arch has a width of one meter and is statically loaded with its self-weight and filling material. Additionally, a gradually increasing live load up to collapse is applied at quarter span. The specific weight of the masonry is 20 kN/m³ while that of the backfill is 15 kN/m³. The friction coefficient used for the simulation is taken directly from the author as $\tan\phi = 0.75$. In ALMA 2.0 the live load at quarter span is simulated by increasing the self-weight of one block as a function of collapse multiplier α, as shown in Fig. 1, whereas the backfill is modelled utilizing concentrated forces applied to the block joints. Simulation of the reinforcement is achieved through the increased value of the cohesion at specific joints where the strengthening measure is placed. In [12] the reinforcement is applied to the joints in between blocks 0 and 14 (see Fig. 1).

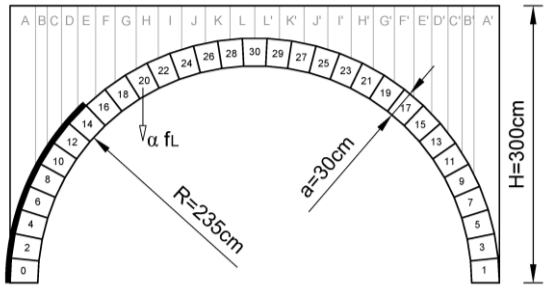

Fig. 1: Arch geometry and loading conditions for EX_1 reproduced from Orduña **[13]**.

The resulting ultimate loads reported by Orduña [13], Baraldi et al. [12] and ALMA 2.0 are given inTable 1. For the unreinforced scenario, Orduña reported an ultimate load value of 18 kN which was obtained through a LA approach, while Baraldi et al. obtained similar results for the FEM approach and slightly lower values for the DEM and Analytical approaches. The value obtained with LA in ALMA 2.0 was 19.67 kN, which corresponds to a value 9.27 % higher than the reference collapse load (18 kN).The linearized case of LA (considering dilatancy instead of friction) gives an overestimation of the collapse multiplier, thus the collapse load [9].

Table 1: Collapse load (in kN) comparison for the EX_1 arch.

Scenario	**LA Orduña**	**DEM Baraldi et al.**	**FEM Baraldi et al.**	**Analytical Baraldi et al.**	**LA ALMA 2.0**
Unreinforced	18.00	18.00	17.80	17.77	19.67
Reinforced	-	22.00	20.75	23.19	26.84

In terms of the collapse mechanism there is also a slight difference between the mechanism reported by Orduña and the one obtained by ALMA 2.0 for the unreinforced scenario. As can be observed in Fig. 2, hinges H1, H2 and H4 are located at the same location for both cases. On the other hand, hinge H3 appears between blocks 13 and 15 (see Fig. 1) in the reference example whereas hinge H3 appears between blocks 21 and 23 (see Fig. 1) for the ALMA 2.0 result. These slight differences found between ALMA 2.0 and the results reported in [13] are probably caused by the modelling choice done by Orduña of dividing the block where the concentrated load is applied (see Fig. 2 (a)). Thus, causing the hinge H2 to appear exactly at quarter span and leading to the appearance of hinge H3 at a different location resulting in a smaller ultimate load.

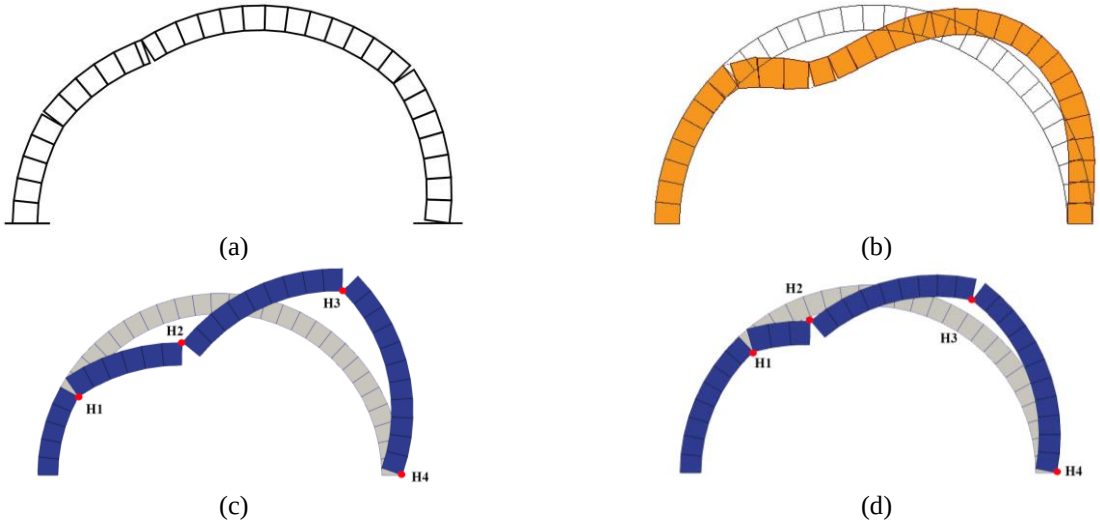

Fig. 2: Collapse mechanisms comparison for the unreinforced arch (a) Orduña **[13]**, (c) ALMA 2.0 and the reinforced arch (b) Baraldi et al. **[12]**, (d) ALMA 2.0.

The collapse mechanism reported by Baraldi et al. and the one obtained with ALMA 2.0 for the reinforced scenario are in perfect agreement. Nevertheless, the difference between collapse load values increased under this scenario, reaching a 29.35 % higher value with ALMA 2.0 in comparison to the value reported for the FEM model of Baraldi et al. Finally, it is worth noting that with the increase of the cohesion value in the joints, where reinforcement is applied, the location of hinges H1 and H2 is shifted providing a higher ultimate load. After reaching a cohesion value of 0.14 N/mm², the collapse load and collapse mechanism are stabilized in the sense that further cohesion increments result in the same load and mechanism. This observation is shown in Fig. 3, where a linear correlation between cohesion and collapse load can be observed. For cohesion values ranging from 0.00 up to 0.14 N/mm2. Higher cohesion values result in a constant collapse load.

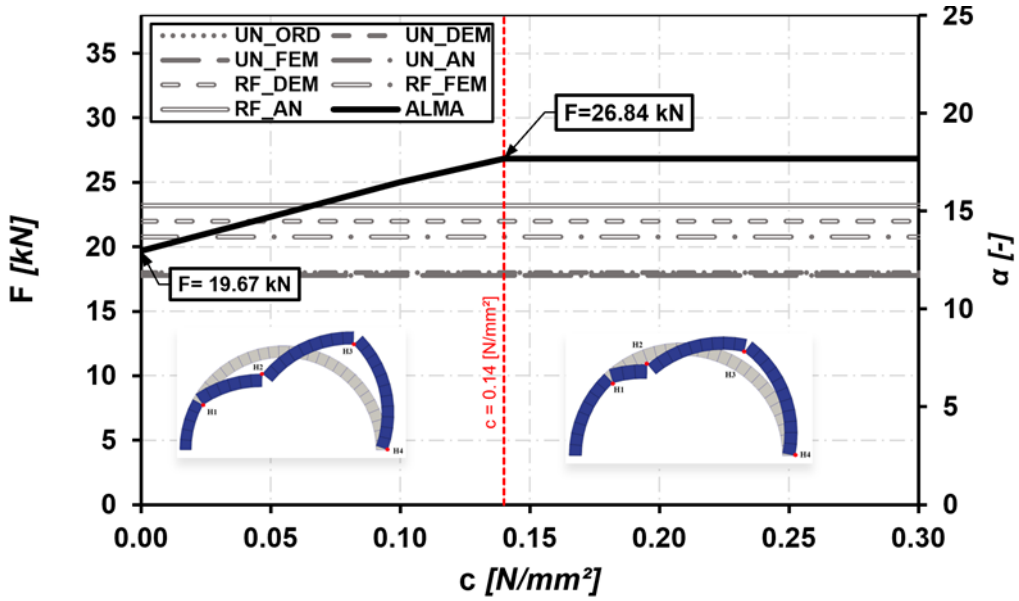

Fig. 3: Collapse load (**F**) and collapse multiplier (**α**) as a function of the cohesion value (**c**) adopted for the unreinforced (**UN**) and reinforced (**RF**) EX_1 arches.

EX_2 – Example 2 from Oliveira et al. [11]

The second example (EX_2) studied in this paper corresponds to the segmental arch experimentally tested by Oliveira et al. [11]. This arch comprises an embrace angle of 156 degrees and is divided into 59 voussoirs that form a single ring. It has an internal radius of 75 cm, with a width of 45 cm and a ring thickness of 5 cm. Two extra blocks have been added to act as the supports for the arch which is subjected to its own self-weight plus a pointed load applied at quarter span. The live load at quarter span in ALMA 2.0 is similarly simulated by increasing the self-weight of one block as a function of collapse multiplier α, as shown in Fig. 4. The unreinforced scenario corresponds to arches US1 and US2 (as per the terminology implemented by Oliveira et al), whereas the reinforced scenario is based on the localized strengthening arrangement of arches LS1 and LS2. Joints between the blocks that have been filled with a grey color (see Fig. 4) are the ones that have been assigned an increased cohesion value to simulate the effect of composite reinforcement.

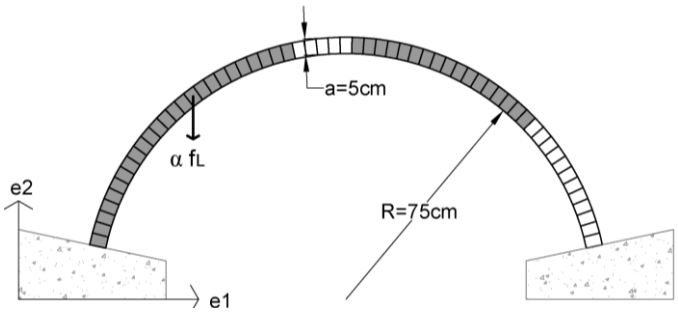

Fig. 4: Arch geometry and loading conditions for EX_2 reproduced from Oliveira et al. **[11]**.

Oliveira et al. reported a minimum, maximum and average values for the collapse load of both unreinforced (US1, US2, US_AVG) and reinforced (LS1, LS2, LS_AVG) arches. The calibration of the ALMA 2.0 models presented in this paper was performed taking the average value as reference which also was in better agreement with the collapsing mechanism related to this load intensity. In order to achieve a good agreement between the reference results and the ones obtained with the ALMA 2.0 model, it was necessary to assign a cohesion value of 6.5 N/mm² to all joints in the model to account for the significant thickness of mortar joints in the experimental model. It must be noted that during the experimental campaign no similarity laws were used for the scaled experimental models which in reality have an important effect on results, especially when dealing with composite materials such as masonry. The large value of cohesion required for the calibration of the model for the unreinforced arch is also related to the fact that the compressive strengths of brick and mortar used in the experimental campaign are almost similar with bricks having only 24% higher compressive strength. Moreover, to calibrate the results for the reinforced scenario, a cohesion value of 27.5 N/mm² was used for the joints reinforced with GFRP (see Table 2) while the rest of the joints were assigned a cohesion value of 6.5 N/mm². The collapse load obtained with ALMA 2.0 for the unreinforced scenario is practically identical to the reference value (only 0.6 % higher). On the other hand, after comparing the collapse loads for the reinforced scenario, the ALMA 2.0 value resulted to be 14.53 % higher than the one obtained by Oliveira et al. The slight difference in load value for the reinforced arch may be due to the strengthening technique used in the experimental campaign, in which two strips of GFRP (8 cm width) were used. In contrast, in ALMA the entire width of the joint is strengthened by increasing the cohesion value assigned.

Table 2: Collapse load comparison for the arch reported by Oliveira et al. **[11]**.

Scenario	Oliveira et al. [kN]	ALMA 2.0 [kN]	c_1^* [N/mm²]	c_2^{**} [N/mm²]
Unreinforced	1.68	1.69	6.50	-
Reinforced	2.96	3.39	6.50	27.50

*cohesion value assigned to the unreinforced joints.
**cohesion value assigned to the reinforced joints

In terms of collapse mechanisms, quite a good agreement was found between the experimental results and the numerical ones obtained with ALMA 2.0. As can be seen in Fig. 5 (a) and (b), all hinges appear in similar locations for the unreinforced scenario, only a shift of one block is observed for hinges H4 and H3. For the reinforced scenario the location of hinges H4, H3 and H1 is identical between the experimental results and those computed with ALMA 2.0. Nonetheless, a shift on hinge location is observed for hinge H2, which instead of developing next to the right extrados composite reinforcement as reported by Oliveira et al., appeared near the end of the intrados reinforcement for the numerical case. This might have occurred since, similarly to EX_1, the hinge H1 of the unreinforced scenario (see Fig. 5 (a) (c)) shifts its position seeking the weak spot, that is found directly after the intrados reinforcement and forms hinge H2 (see Fig. 5 (d)).

In Fig. 6, the influence that cohesion value has in the collapse load is presented. The unreinforced scenario is represented by the cohesion values ranging from 0 up to 6.5 N/mm2. After this range, the cohesion value at the reinforced joints is increased until reaching a value of 27.5 N/mm2. At this

value there is a change in the collapse mechanism obtained and the new mechanism is pretty similar to the one reported from the experimental campaign. After this threshold value, further increments on the cohesion value of the reinforced joints produce the same collapse load and collapse mechanism. In order to simulate the strengthening effect of the composite material, higher values of cohesion have been used to reach a stabilizing collapse load, which is achieved for a value of 27.5 N/mm². This value should be able to represent the collapse mechanism without being affected by the joint cohesion since all the plastic hinges appear outside the strengthened joints and are not influenced by it.

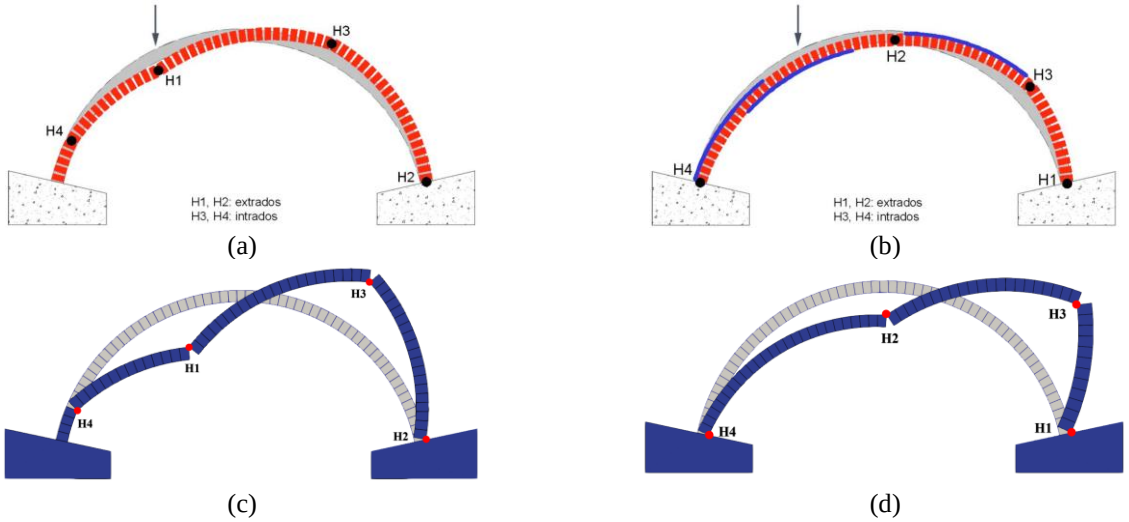

Fig. 5: Collapse mechanisms comparison for the unreinforced case (a) Oliveira et al. **[11]**, (c) ALMA 2.0 and reinforced case (b) Oliveira et al. **[11]**, (d) ALMA 2.0.

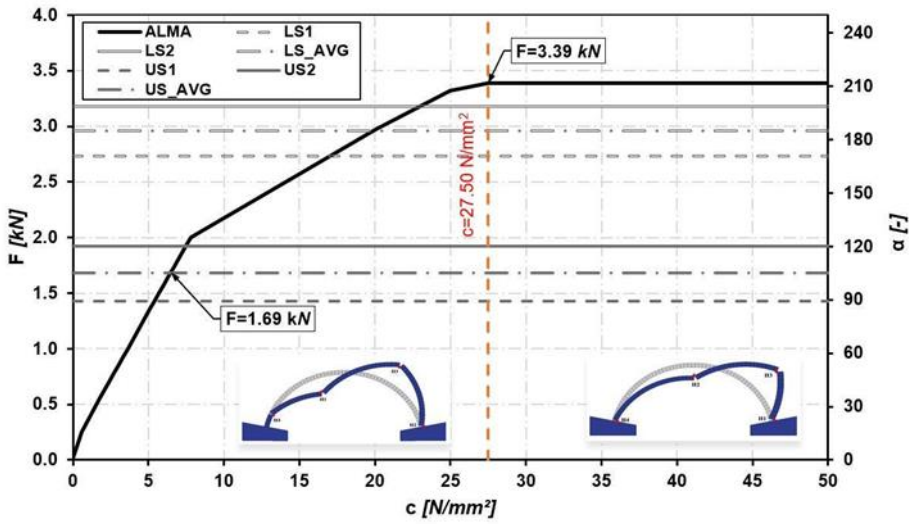

Fig. 6: Collapse load (**F**) and multiplier (**α**) as a function of the cohesion (**c**) value adopted for the unreinforced (**US**) and reinforced (**LS**) EX_2 arches.

Final Remarks

Arches with partial composite reinforcement are the focus of this study in validation of the new enrichment of the inhouse code for LA ALMA 2.0. Two examples are considered from literature as benchmarks for the validation and calibration.

A semi-circular arch with a backfill is studied as the first example that is initially assessed for the unreinforced scenario using LA by [13] and then using FEM, DEM and an analytical approach by [12]. The outcomes of the two studies are in good accordance with ALMA 2.0 where slight discrepancies are observed due to some differences in the original geometry assumptions. Afterwards a partial strengthening technique on the arch extrados of the left support is applied and numerically

modelled in FEM, DEM and analytical, where distinctly this measure is able to shift the collapse mechanism into providing higher values for the collapse load. ALMA 2.0 was able to shift the location of the hinge causing the collapse mechanism, and therefore obtaining a higher collapse load value, by increasing the cohesion value of the joints where the reinforcement is applied. Exact collapse mechanisms are achieved with slight differences in the collapse load values with respect to the values reported in the literature.

The second case study corresponds to a segmental arch for which an extensive experimental campaign on scaled models has been conducted and reported by [11]. ALMA 2.0 simulations of the unreinforced and partially reinforced cases reported by Oliveira et al. where performed. By utilizing different values of cohesion, it was possible to calibrate the collapse load and obtain similar collapse mechanisms as those of the referenced experimental campaign. Relatively large values of cohesion were necessary to reach the experimental load for both cases. This may have been due to the considerable thickness and resistance of the mortar joints of the experimental models. The average collapse load obtained with ALMA 2.0 for the unreinforced scenario was in perfect correspondence with the value reported in [11]. On the other hand, for the reinforced scenario slightly higher collapse loads were obtained with the LA numerical simulations performed.

It has been shown that improvements and enrichments of LA codes, which require few input parameters, could be capable of providing relatively fast and reliable results for the assessment of composite reinforced masonry arches. Nonetheless, finding strategies and techniques to account for the many impacts that follow the complex nature of masonry structures and their behaviour when strengthened remains an active field of research.

References

[1] P. B. Lourenço, “Computations on historic masonry structures,” Progress in Structural Engineering 4, pp. 301-319, 2002.

[2] P. Roca, M. Cervera, G. Gariup and L. Pela, “Structural Analysis of Masonry Historical Constructions. Classical and Advanced Approaches,” Archives of Computational Methods in Engineering 17, pp. 299-325, 2010.

[3] A. M. D' Altri, V. Sarhosis, G. Milani, J. Rots, S. Cattari, S. Lagomarsino, E. Sacco, A. Tralli, G. Castellazzi and S. de Miranda, “Modeling Strategies for the Computational Analysis of Unreinforced Masonry Structures: Review and Classification,” Archives of Computational Methods in Engineering 27, pp. 1153-1185, 2020.

[4] E. Reccia, L. Leonetti, P. Trovalusci and A. Cecchi, “A multi-scale/multi-domain model for the failure analysis of masonry walls: A validation with combined FEM/DEM approach,” Journal for Multiscale Computational Engineering, vol. 16, no. 4, pp. 325-343, 2018.

[5] M. Pepe, M. Pingaro, E. Reccia and P. Trovalusci, “Micromodels for the In-Plane Failure Analysis of Masonry Walls with Friction: Limit Analysis and DEM-FEM/DEM Approaches,” in Conference of 24th Conference of the Italian Association of Theoretical and Applied Mechanics, AIMETA 2019, Rome, 2020.

[6] M. Pepe, M. Pingaro, P. Trovalusci, E. Reccia and L. Leonetti, “Micromodels for the in-plane failure analysis of masonry walls: Limit Analysis, FEM and FEM/DEM appraoches,” Frattura ed Integrità Strutturale, vol. 51, pp. 356-368, 2020.

[7] M. Pepe, M. Sangirardi, E. Reccia, M. Pingaro, P. Trovalusci and G. de Felice, “Discrete and Continuous Approaches for the Failure Analysis of Masonry Structures Subjected to Settlements,” Frontiers in Built Environment, vol. 6, no. 43, 2020.

[8] M. Pepe, “Numerical modeling for masonry: ALMA 2.0, A computational code for the limit analysis of historical masonry structures,” Ph.D. thesis, Sapienza University of Rome, Rome, 2020.

[9] C. Baggio and P. Trovalusci, “Collapse behaviour of three-dimensional brick-block systems using non-linear programming,” Structural Engineering and Mechanics, vol. 10, no. 2, pp. 181-195, 2000.

[10] I. Cancelliere, M. Imbimbo and E. Sacco, “Experimental tests and numerical modeling of reinforced masonry arches,” Engineering Structures, vol. 32, no. 3, pp. 776-792, 2010.

[11] D. V. Oliveira, I. Basilio and P. B. Lourenço, “Experimental Behavior of FRP Strengthened Masonry Arches,” Journal of Composites for Construction, vol. 14, no. 3, pp. 312-322, 2010.

[12] D. Baraldi, G. Boscato, C. B. De Carvalho Bello, A. Cecchi and E. Reccia, “Discrete and Finite Element Models for the Analysis of Unreinforced and Partially Reinforced Masonry Arches,” Key Engineering Materials, vol. 817, pp. 229-235, 2019.

[13] A. Orduña, “Seismic Assessment of Ancient Masonry Structures by Rigid Blocks Limit Analysis,” Ph.D. thesis, University of Minho, Guimarães, 2004.